

Electron $g - 2$ corrections from axion dark matter

Ariel Arza^{1,*} and Jason L. Evans^{1,†}

¹*Tsung-Dao Lee Institute, Shanghai Jiao Tong University, Shanghai 200240, China*

(Dated: October 2, 2024)

We consider the effects of a local axion dark matter background on the $g - 2$ of the electron. We calculate loop corrections to the photon-electron vertex and determine analytical formulas for the spin and cyclotron frequencies when the electron is in an external magnetic field. By comparing with current measurements of these observables, we are able to place the strongest constraint on the axion-electron coupling for axion masses below 3×10^{-18} eV.

I. INTRODUCTION

The identity of dark matter is currently one of the most debated puzzles in all of natural science. The QCD axion [1–5] and axion-like particles (ALPs) [6, 7] are among the leading candidates [8–11]. Axions are commonly searched for by looking at their interaction with photons, especially axion to photon conversions in strong external magnetic fields [12]. See Refs. [13] and [14] for recent reviews on axion phenomenology.

For axion-electron interactions, strong constraints are placed on masses between 0.1 and 10 keV by the underground electron recoil experiments such as XENON1T [15] and XENONnT [16], while for masses above 10 keV, strong constraints are from radiative decays of axion dark matter via a one loop electron diagram [17]. For masses below 0.1 keV, the constraints on the axion-electron coupling g_{ae} are dominated by the resulting energy loss of red-giant branch stars, which has been updated to $g_{ae} < 1.3 \times 10^{-13}$ [18].

In this work we constrain the axion dark matter interaction with the electron by computing the effects of a cold axion background on the electron magnetic dipole moment. As it was pointed out recently in [19], ultra light bosonic dark matter corrects the value of $g - 2$ of the electron substantially due to the high occupancy number of the background field. It was shown that the corrections become larger for lower masses, allowing for a constraint on the dark photon kinetic mixing parameter of $\chi < 7.1 \times 10^{-11} \left(\frac{m_{\gamma'}}{10^{-14} \text{ eV}} \right)$. This being the strongest constraints on dark photon dark matter for a dark photon masses $m_{\gamma'}$ below 10^{-14} eV.

In the same spirit, we expect constraints on the axion-electron coupling. We could estimate a constraint to the axion-electron coupling from the naive mapping $\chi \leftrightarrow g_{ae}$. However, as scalar have zero spin, the $g - 2$ corrections should be suppressed by the axion velocity. As shown in our results, we get the constraint to be $g_{ae} \lesssim 4.48 \times 10^{-30} (m_a/\text{eV})$, which is competitive with current constraints for masses close to 10^{-17} eV, and becomes even stronger for lower masses. We also take this op-

portunity to include in our analysis other dark matter candidates with a standard Yukawa type interaction.

This article is organized as follows: in Sec. II we discuss the formalism for the loop correction inspired by QFT techniques at finite temperature and give a fairly general discussion on the corrections to the electron-photon vertex in the presence of a background. In Sec. III, we apply this formalism for the case of an axion dark matter background. We consider axions with both a derivative term interaction and also a pseudoscalar Yukawa interaction with the electron¹. We also consider a dark scalar interacting with a Yukawa coupling. In Sec. IV we compute the cyclotron and spin frequency of an electron in a uniform magnetic field, and compare our results with an updated measurement of these observables in a penning trap. We finally conclude in Sec. V.

II. LOOP CORRECTIONS FORMALISM

The zeroth order contribution to the electron magnetic moment arises from the fermion-photon vertex in quantum electrodynamics (QED). The one loop corrections to the classical QED theory provide a contribution given by $g - 2 = \alpha/\pi$, where α is the fine structure constant. For this case, the loops only involve virtual photons.

One can, of course, include corrections from beyond SM particles that interact with the electron. For example, for virtual scalar or pseudoscalar particles with interaction couplings g_{ae} , the contributions to the anomalous magnetic moment are of the order of $g - 2 \sim \frac{g_{ae}^2}{16\pi^2}$. This is too small even for comparison with the highest precision measurements. Indeed, the values of g_{ae} that gives a $g - 2$ contribution comparable with current uncertainties, are already constrained by many other experiments and observations (See Sec. I).

However, if these scalar or pseudoscalar particles are not virtual particles but are instead real non-relativistic particles of the background, things are different. Based

* ariel.arza@gmail.com

† jlevans@sjtu.edu.cn

¹ Although in the literature both interaction are considered as equivalent, this is only guaranteed to be true for on-shell vertices.

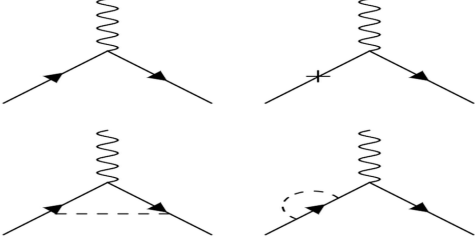


FIG. 1. Relevant diagrams for our computations. The dashed lines correspond to the dark matter background states.

on the work [19], we anticipate that the $g - 2$ correction picks up a factor of order $\frac{\rho_a}{m_a^2 m_e^2}$ with respect to the case with virtual particles where m_e is the electron mass, m_a the dark matter candidate mass and ρ_a its local energy density. Assuming that these particles make up all the dark matter energy density, i.e. $\rho_a = 0.3 \text{ GeV/cm}^3$ for the standard halo model, this additional factor results in an enhancement with respect to the virtual particle case, if m_a is below $\sim 10^{-9} \text{ eV}$.

For calculating the dark matter background effects we base our analysis on the techniques discussed in Refs. [20, 21] for QED at finite temperature and [19] for a dark matter background. In a background, the propagator of a scalar or pseudoscalar dark matter field is corrected in the same way it is in finite temperature,

$$\Delta_F(q) = \frac{1}{q^2 - m_a^2 + i\epsilon} - 2\pi i f_a(q) \delta(q^2 - m_a^2) \quad (1)$$

except $f_a(q)$ is the occupancy number of the background dark matter field not one of the standard thermal equilibrium distributions.

The electron self-energy for a particular momentum $k^\mu \equiv (E, \vec{k})$ is now $\Sigma(k) = \Sigma_0(k) + \Sigma_\beta(k)$, where $\Sigma_0(k)$ corresponds to the electron self-energy in the vacuum and $\Sigma_\beta(k)$ the background contribution. The latter can be expressed in general terms as

$$\Sigma_\beta(k) = B(k) + C(k)(\not{k} - m_e) + \not{D}(k) \quad (2)$$

where B , C and D_μ are functions determined by the type of interactions we are considering. They are written in detailed in Sec. III. The form of this correction to the electron self-energy highlights the fact that the background gives a preferred frame and so violates Lorentz invariance. Without this violation, $\not{D}(k)$ would be proportional to \not{k} and would contribute to the standard wave function and mass renormalization. However, because of this term, the background corrects the spinor dynamics in a non-trivial way,

$$(\not{k} - m_e + \Sigma_\beta(k))u_\beta(k, s) = 0, \quad (3)$$

with spinors which are normalized in the usual way $u_\beta(k, s)^\dagger u_\beta(k, s') = \delta_{ss'}$. Writing $\not{k} - m_e + \Sigma_\beta(k) = \not{\tilde{k}} -$

\tilde{m}_e , the spin sums are now $\sum_s u_\beta(k, s)\bar{u}_\beta(k, s) = \frac{\not{\tilde{k}} + \tilde{m}_e}{E}$ and $\sum_s v_\beta(k, s)\bar{v}_\beta(k, s) = \frac{\not{\tilde{k}} - \tilde{m}_e}{E}$.

As is clear from this discussion, the wave function is of course renormalized by the background as well. The renormalized Feynman propagator takes on the usual form

$$S_F^R(x - x') = \int \frac{d^4 k}{(2\pi)^4} e^{-ik \cdot (x - x')} \frac{Z_2^{-1}}{\not{\tilde{k}} - \tilde{m}_e + i\epsilon} \quad (4)$$

where Z_2 is the wave function renormalization constant. On the other hand, the renormalized propagator can also be found as follows

$$\begin{aligned} S_F^R(x - x') &= -i \langle 0 | T[\psi_e(x)\bar{\psi}_e(x')] | 0 \rangle \\ &= -i \int \frac{d^3 k}{(2\pi)^3} \left(\Theta(t - t') \frac{\not{\tilde{k}} + \tilde{m}_e}{2\tilde{E}} e^{-ip \cdot (x - x')} \right. \\ &\quad \left. - \Theta(t' - t) \frac{\not{\tilde{k}} - \tilde{m}_e}{2\tilde{E}} e^{ip \cdot (x - x')} \right). \end{aligned} \quad (5)$$

Comparing Eq. (4) with Eq. (5), gives the following definition of wave function renormalization

$$Z_2(k) = 1 - C(k) - \frac{m_e}{E} \frac{d}{dE} \left(B(k) + \frac{k \cdot D(k)}{m_e} \right) + \frac{D_0(k)}{2E}. \quad (6)$$

Now we can compute all the contributions to the electron anomalous magnetic moment. The relevant diagrams are specified in Fig. 1. The counterterm diagrams are necessary because of the modification to the free propagation of the electron in the dark matter background. Assuming a spherically symmetric dark matter distribution $f(q)$, the total vertex, i.e. the sum of the diagrams shown in Fig. 1, can be computed in general terms as in Ref. [19] to give

$$\begin{aligned} i\mathcal{M}_\mu^{\text{total}}(k, k') &= (-ie)\bar{u}(k')(\gamma_\mu + Q_\mu(k) + Q_\mu(k')) \\ &\quad + \frac{i}{2}\sigma_{\nu\rho} \frac{\Delta k^\rho}{2m_e} \left(\frac{dD^\nu}{dk^\mu} + \frac{dD^\nu}{dk'^\mu} \right) \\ &\quad + F_\mu(k, \Delta k) u(k). \end{aligned} \quad (7)$$

Here $\Delta k_\mu = k'_\mu - k_\mu$, $\sigma_{\mu\nu} = \frac{i}{2}[\gamma_\mu, \gamma_\nu]$ and $Q_\mu(k)$ is defined as

$$\begin{aligned} Q_\mu(k) &= \frac{1}{2} \left(\frac{d}{dk^\mu} - \frac{m}{E_k} \frac{d}{dE} \right) \left(B(k) + \frac{k \cdot D(k)}{m_e} \right) \\ &\quad + \gamma_\mu \frac{D_0(k)}{2E_k} - \frac{D_\mu(k)}{2m_e}, \end{aligned} \quad (8)$$

where $E_k = \sqrt{k^2 + m_e^2}$. the function $F_\mu(k, \Delta k)$ appears from the bottom-left diagram in Fig. 1 and is the only part on Eq. (7) that depends on the particle dark matter model considered. It will be made explicit in Sec. III.

To conclude this section we want to shortly discuss the scaling of the expected results. As the electron $g - 2$

corrections due to a dark matter background are proportional to the dark matter occupancy number $f_a(q)$, and as the occupancy number for non-relativistic particles scales as $f_a \sim 1/m_a^4$, in general one would also expect terms of this type in Eq. (7). However, those terms correspond to the analogous of IR divergences. At the end of the day, these contributions from the different diagrams cancel out and the final results are terms that scale at most as $\sim 1/m_a^2$. These cancellations are general properties of finite temperature loop calculations and were also discussed in Refs. [20, 21]. Now, our final results that scale as $\sim 1/m_a^2$ still show a divergence as $m_a \rightarrow 0$, however it is a physical consequence of the scaling of the occupancy number, i.e., $f_a \sim 1/m_a^4$, which diverge very fast as $m_a \rightarrow 0$. In refs. [20, 21] this physical divergence does not appear because they consider a photon thermal distribution where the occupancy number diverge as $f_\gamma \sim 1/|\vec{q}|$ for $|\vec{q}| \rightarrow 0$, not as fast as the cold dark matter occupancy number. Another possible issue is that for very small masses perturbation theory breaks down. However, this is not the case for the parameter space we are considering.

III. ANALYTICAL RESULTS FOR (PSEUDO)SCALAR DARK MATTER MODELS

We consider three different interactions, an axion with a derivative coupling to fermions, a pseudoscalar with a Yukawa type interaction (pYukawa) and a scalar with a Yukawa coupling (sYukawa). Our interaction Lagrangian has the form

$$\mathcal{L}_I = \frac{g_{ae}^{(d)}}{2m_e} \partial_\mu a \bar{\psi} \gamma^\mu \gamma_5 \psi + g_{ae}^{(p)} a \bar{\psi} i \gamma_5 \psi + g_{ae}^{(s)} a \bar{\psi} \psi. \quad (9)$$

We consider, initially, that only one of these candidates make 100% of the dark matter and denote their couplings simply by g_{ae} . First, we write the coefficients of the fermion self-energy defined in Eq. (2),

$$B(k) = -g_{ae}^2 \int \frac{d^4 q}{(2\pi)^3} f_a(q) \delta(q^2 - m_a^2) \frac{m(b_0 + b_2 R)}{(k+q)^2 - m_e^2} \quad (10)$$

$$C(k) = -g_{ae}^2 \int \frac{d^4 q}{(2\pi)^3} f_a(q) \delta(q^2 - m_a^2) \frac{c_0 + c_2 R}{(k+q)^2 - m_e^2} \quad (11)$$

$$D_\mu(k) = -g_{ae}^2 \int \frac{d^4 q}{(2\pi)^3} f_a(q) \delta(q^2 - m_a^2) \frac{(d_0 + d_2 R + \bar{d} \frac{k \cdot q}{m_e^2}) q_\mu}{(k+q)^2 - m_e^2} \quad (12)$$

where $R = m_a^2/m_e^2$. The values of the coefficients $\{b_i, c_i, d_i\}$ and \bar{d} depend on whether the dark matter has a derivative, pYukawa or sYukawa interaction with fermions. They are given in Table I.

TABLE I.

interaction	b_0	b_2	c_0	c_2	d_0	d_2	\bar{d}
derivative	0	$\frac{1}{2}$	0	$\frac{1}{4}$	0	$-\frac{1}{4}$	$-\frac{1}{2}$
pYukawa	0	0	1	0	1	0	0
sYukawa	2	0	1	0	1	0	0

The function $F_\mu(k, \Delta k)$ has the form

$$F_\mu(k, \Delta k) = \frac{\Delta k^\nu}{2m_e} \left(-\gamma_\mu \left(\frac{b_2}{2} I_\nu(k) + \frac{d_0}{2} R \bar{I}_\nu(k) \right) - i \sigma_{\mu\nu} \left(\frac{b_2}{2} \bar{I}(k) + \frac{d_0}{2} R \bar{I}(k) \right) - \frac{b_0}{2} \left(I_A(k) + \frac{3}{4} R^2 \bar{I}_A(k) \right) - i \frac{\bar{d}}{2} \gamma^\alpha \sigma_{\mu\nu} \gamma^\beta I_{\alpha\beta}(k) \right), \quad (13)$$

where the functions $I_A(k)$, $J_A(k)$, $I_\mu(k)$, $\bar{I}_\mu(k)$ and $I_{\mu\nu}(k)$ are defined as

$$J(k) = \frac{g_{ae}^2}{m_e^2} \int \frac{d^4 q}{(2\pi)^3} f_a(q) \delta(q^2 - m_a^2), \quad (14)$$

$$I_A(k) = g_{ae}^2 \int \frac{d^4 q}{(2\pi)^3} f_a(q) \delta(q^2 - m_a^2) \frac{m_e^2}{(q \cdot k)^2}, \quad (15)$$

$$\bar{I}_A(k) = g_{ae}^2 \int \frac{d^4 q}{(2\pi)^3} f_a(q) \delta(q^2 - m_a^2) \frac{m_e^6}{(q \cdot k)^4}, \quad (16)$$

$$I_\mu(k) = \frac{g_{ae}^2}{m_e} \int \frac{d^4 q}{(2\pi)^3} f_a(q) \delta(q^2 - m_a^2) \frac{q_\mu}{q \cdot k}, \quad (17)$$

$$\bar{I}_\mu(k) = g_{ae}^2 \int \frac{d^4 q}{(2\pi)^3} f_a(q) \delta(q^2 - m_a^2) \frac{m_e^3 q_\mu}{(q \cdot k)^3}, \quad (18)$$

$$I_{\mu\nu}(k) = g_{ae}^2 \int \frac{d^4 q}{(2\pi)^3} f_a(q) \delta(q^2 - m_a^2) \frac{q_\mu q_\nu}{(q \cdot k)^2}. \quad (19)$$

IV. PHENOMENOLOGY

In this section we translate our results into measured quantities. We take the most up-to-date measurement of the electron $g-2$ found in Ref. [22] and use it to place constraints on the coupling to the electron of the dark matter candidates considered. The quantity which is actually measured in Refs. [22, 23] is $\omega_a = (\omega_c - \omega_s)$, which ratio ω_a/ω_c directly corresponds to the value of $(g-2)/2$. The experimental results of [22] are in agreement with the standard model prediction to about

$$\delta_E \left(\frac{\omega_s - \omega_c}{\omega_c} \right) = 0.7 \times 10^{-12}. \quad (20)$$

For our case, however, the strongest constraints can be determined by comparing our result with the experimental error obtained for ω_a . From figure 4.27 of [23] this

error is set to be

$$\frac{\delta_E \omega_a}{\omega_a} = 4.3 \times 10^{-12}. \quad (21)$$

Any dark matter correction for ω_a that surpass this value will be constrained².

To determine ω_c and ω_s from our loop correction, we must first find the resulting Hamiltonian for the case of an electron motion in a static and homogeneous magnetic field \vec{B} . The electron dynamics is then described by the following equation of motion

$$\begin{aligned} & (\not{k} - m_e + B(k) + \not{D}(k) - eA^\mu(\gamma_\mu + 2Q_\mu(k)) \\ & + i\sigma_{\nu\rho} \frac{\Delta k^\rho}{2m_e} \frac{dD^\nu}{dk^\mu} + F_\mu(k, \Delta k)) u(k, s) = 0, \end{aligned} \quad (22)$$

where A^μ is the electromagnetic vector potential, which has a vanishing zero component A_0 and is related to the magnetic field by $\vec{A} = \frac{1}{2}\vec{B} \times \vec{r}$. The Hamiltonian is obtained by solving this equation for k_0 .

With the definitions $\rho_1 = -\gamma_5$, $\rho_2 = i\gamma_0\gamma_5$ and $\rho_3 = \gamma_0$, the Hamiltonian takes the form

$$H = -\rho_1 \vec{\sigma} \cdot \vec{\pi} + \rho_3 (\bar{m}_e + S_+ + S_-) - D_0. \quad (23)$$

Here $\bar{m}_e = m_e - B$, σ_i are the Pauli matrices and $\vec{\pi}(k) = \vec{k} - e\vec{A}G(k)$, where $G(k) = 1 + \frac{D_0(k)}{E_k} + b_0 m_e R \frac{\bar{I}_0(k)}{2E_k}$. S_+ (S_-) is an operator that commute (anticommute) with ρ_2 . They are defined as $S_+ = -\frac{e}{2m_e} \partial^j A^i \sigma_{ij} h_+$ and $S_- = \frac{e}{2m_e} \partial^j A^i \left(\rho_3 \sigma_{ij} h_-^{(1)} - i \frac{k_i}{2m_e} \rho_1 \sigma_j h_-^{(2)} \right)$, where $h_+ = -\frac{\bar{d}}{2} J + \frac{d_0 - b_2}{2} R I_A - d_2 I_{00} + (d_0/2 + d_2) I_i^i/3$, $h_-^{(1)} = \frac{b_2}{2} I_0 + \frac{d_0}{2} R \bar{I}_0$ and $h_-^{(2)} = -\bar{d} I_0 + d_0 R \bar{I}_0$. This result was found under the assumption of a spherically symmetric dark matter distribution, then terms of the form \bar{I}_i , I_i and I_{0i} are zero.

To diagonalize the Hamiltonian (see section IV in [20]), we perform a rotation

$$H' = e^{-\frac{i}{2}\phi\rho_2} H e^{\frac{i}{2}\phi\rho_2} \quad (24)$$

such that

$$\tan(\phi) = \frac{\vec{\sigma} \cdot \vec{\pi}}{\bar{m}_e}. \quad (25)$$

After some algebra, we get

$$\begin{aligned} H' = & E_\beta - \frac{e}{2E_\beta} \left(1 + b_0 m_e R \frac{\bar{I}_0}{2E_k} \right) \vec{L} \cdot \vec{B} \\ & - \frac{e}{2E_\beta} \left(1 + b_0 m_e R \frac{\bar{I}_0}{2E_k} + \frac{E_k}{m_e} h_+ \right. \\ & \left. - h_-^{(1)} - \frac{k^2}{4m_e^2} h_-^{(2)} \right) \vec{\sigma} \cdot \vec{B}, \end{aligned} \quad (26)$$

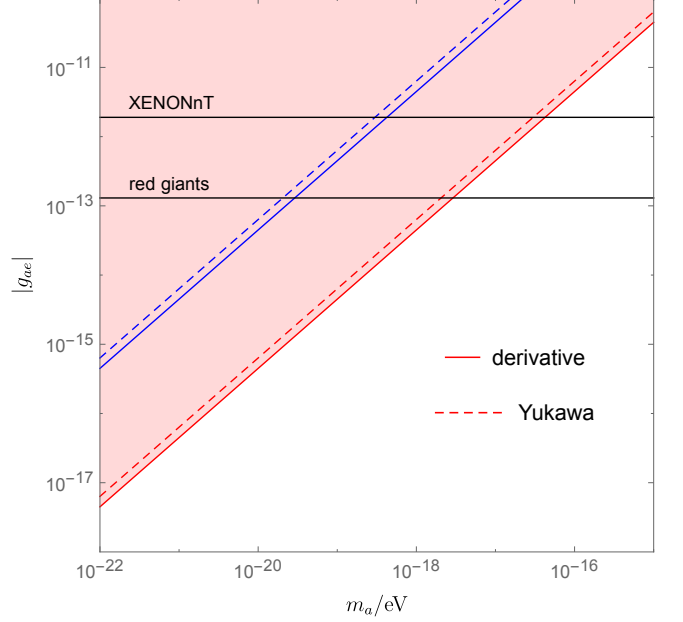


FIG. 2. Constraints on the axion-electron coupling. The solid red line corresponds to constraints obtained in this work for the case of a derivative coupling while the dashed red line stands for the case of a pseudoscalar Yukawa coupling. The solid and dashed blue lines are constraints for the derivative and Yukawa p-scalar coupling, respectively, assuming the local axion energy density is just a 0.01% of the total dark matter. The solid black lines are current constraints from solar axions (XENONnT) and red giant evolution.

where \vec{L} is the electron angular momentum and $E_\beta = \sqrt{k^2 + m_\beta^2}$, with m_β the physical mass that the electron acquires from the background. It is given by

$$m_\beta = m_e - B - \frac{E_k}{m_e} D_0. \quad (27)$$

The cyclotron and spin frequencies are the factors that multiply \vec{L} and $\vec{\sigma}$, respectively, in Eq. (26), giving

$$\omega_c = \frac{eB}{2E_\beta} \left(1 + b_0 m_e R \frac{\bar{I}_0}{2E_k} \right) \quad (28)$$

$$\omega_s = \omega_c \left(1 + \frac{\alpha}{2\pi} \frac{E_k}{m_e} + \frac{E_k}{m_e} h_+ - h_-^{(1)} - \frac{|\vec{k}|^2}{4m_e^2} h_-^{(2)} \right). \quad (29)$$

Note, we have added the one-loop quantum electrodynamics contribution for zero background.

Now we perform the integrals defined in Eqs. (15)-(19) and input the results into Eqs. (28) and (29). Using the non-relativistic properties of the dark matter background, we evaluate the integrals after we expand the integrands to second order in the dark matter and electron velocities.

² A more conservative estimate of this error will have a minimal effect on our results since the constraints scale as the square root of the error.

Defining

$$\lambda = \frac{g_{ae}^2 \rho_a}{m_a^2 m_e^2}, \quad (30)$$

and the dark matter and electron velocities as v_a and v_e , respectively, our dark matter background corrections to the parameter ω_a reduce to the following expressions

$$\frac{\delta_T \omega_a}{\omega_a} = \frac{2\pi}{\alpha} \begin{cases} \lambda \left(\frac{1}{3} \langle v_a^2 \rangle + \frac{1}{8} v_e^2 \right) & \text{derivative} \\ \lambda \left(-\frac{1}{6} \langle v_a^2 \rangle + \frac{1}{4} v_e^2 \right) & \text{pYukawa/sYukawa} \end{cases}, \quad (31)$$

where $\langle \rangle$ means averaging over the dark matter velocity distribution.

To compare with Eq. (21) we need an idea of the value of v_e in the experiment. The velocity of the electron in the trap are of the order of $v_e \sim 2.3 \times 10^{-4} c$ [22]. As this value is smaller than the dark matter standard average velocity, namely $\sqrt{\langle v_a^2 \rangle} = 270 \text{ km/s}$, we neglect the electron velocity contribution.

Making our theoretical predictions in Eq. (31) to be smaller than the experimental error given in Eq. (21), our constraints are

$$g_{ae} < \begin{cases} 4.48 \times 10^{-14} \left(\frac{m_a}{10^{-18} \text{ eV}} \right) & \text{derivative} \\ 6.34 \times 10^{-14} \left(\frac{m_a}{10^{-18} \text{ eV}} \right) & \text{pYukawa/sYukawa} \end{cases} \quad (32)$$

In Fig. 2, we compare our constraints for the derivative and pYukawa coupling with the strongest currents constraints. We see that ours are competitive or stronger for masses below $m_a = 3 \times 10^{-18} \text{ eV}$. For the scalar case, very strong constraints, i.e. $g_{ae} < 10^{-24}$ and 10^{-25} , are given by tests of the equivalency principle [24, 25]. For masses below $m_a = 10^{-18} \text{ eV}$, there are even stronger constraints for scalar dark matter candidates [26–28]. Thus, for the sYukawa case our results are of no effect.

V. CONCLUSION

In this work we have discussed the effects of a pseudoscalar and scalar dark matter background on the electron $g - 2$ value. We have performed loop corrections on the electron-photon vertex using techniques similar to those found in finite temperature field theory. These same techniques were used to perform a similar calculation on the dark photon dark matter case discussed in [19]. Taking the most up-to-date measurements of these observables, we were able to place the strongest constraints on axion-like dark matter for axion masses below $3 \times 10^{-18} \text{ eV}$. For the case of scalar dark matter, our results are not competitive with current constraints from equivalence principle tests.

ACKNOWLEDGEMENT

We would like to thank Tsutomu T. Yanagida and Xing Fan for useful discussions regarding this work.

-
- [1] R. D. Peccei and H. R. Quinn, *CP Conservation in the Presence of Instantons*, *Phys. Rev. Lett.* **38** (1977) 1440–1443.
- [2] J. E. Kim, *Weak Interaction Singlet and Strong CP Invariance*, *Phys. Rev. Lett.* **43** (1979) 103.
- [3] M. A. Shifman, A. I. Vainshtein and V. I. Zakharov, *Can Confinement Ensure Natural CP Invariance of Strong Interactions?*, *Nucl. Phys. B* **166** (1980) 493–506.
- [4] M. Dine, W. Fischler and M. Srednicki, *A Simple Solution to the Strong CP Problem with a Harmless Axion*, *Phys. Lett. B* **104** (1981) 199–202.
- [5] A. R. Zhitnitsky, *On Possible Suppression of the Axion Hadron Interactions. (In Russian)*, *Sov. J. Nucl. Phys.* **31** (1980) 260.
- [6] P. Svrcek and E. Witten, *Axions In String Theory*, *JHEP* **06** (2006) 051 [arXiv:hep-th/0605206].
- [7] A. Arvanitaki, S. Dimopoulos, S. Dubovsky, N. Kaloper and J. March-Russell, *String Axiverse*, *Phys. Rev. D* **81** (2010) 123530 [arXiv:0905.4720].
- [8] J. Preskill, M. B. Wise and F. Wilczek, *Cosmology of the Invisible Axion*, *Phys. Lett. B* **120** (1983) 127–132.
- [9] L. Abbott and P. Sikivie, *A Cosmological Bound on the Invisible Axion*, *Phys. Lett. B* **120** (1983) 133–136.
- [10] M. Dine and W. Fischler, *The Not So Harmless Axion*, *Phys. Lett. B* **120** (1983) 137–141.
- [11] P. Arias, D. Cadamuro, M. Goodsell, J. Jaeckel, J. Redondo and A. Ringwald, *WISPy Cold Dark Matter*, *JCAP* **06** (2012) 013 [arXiv:1201.5902].
- [12] P. Sikivie, *Experimental Tests of the Invisible Axion*, *Phys. Rev. Lett.* **51** (1983) 1415–1417.
- [13] P. Sikivie, *Invisible Axion Search Methods*, *Rev. Mod. Phys.* **93** (2021) 015004 [arXiv:2003.02206].
- [14] I. G. Irastorza and J. Redondo, *New experimental approaches in the search for axion-like particles*, *Prog. Part. Nucl. Phys.* **102** (2018) 89–159 [arXiv:1801.08127].
- [15] XENON, E. Aprile et al., *Light Dark Matter Search with Ionization Signals in XENON1T*, *Phys. Rev. Lett.* **123** (2019) 251801 [arXiv:1907.11485].
- [16] XENON, E. Aprile et al., *Search for New Physics in Electronic Recoil Data from XENONnT*, *Phys. Rev. Lett.* **129** (2022) 161805 [arXiv:2207.11330].
- [17] R. Z. Ferreira, M. C. D. Marsh and E. Müller, *Do Direct Detection Experiments Constrain Axionlike Particles Coupled to Electrons?*, *Phys. Rev. Lett.* **128** (2022) 221302 [arXiv:2202.08858].

- [18] F. Capozzi and G. Raffelt, *Axion and neutrino bounds improved with new calibrations of the tip of the red-giant branch using geometric distance determinations*, *Phys. Rev. D* **102** (2020) 083007 [[arXiv:2007.03694](#)].
- [19] J. L. Evans, *Effect of Ultralight Dark Matter on $g - 2$ of the Electron*, [arXiv:2302.08746](#).
- [20] J. F. Donoghue, B. R. Holstein and R. W. Robinett, *QUANTUM ELECTRODYNAMICS AT FINITE TEMPERATURE*, *Annals Phys.* **164** (1985) 233.
- [21] J. F. Donoghue and B. R. Holstein, *Renormalization and Radiative Corrections at Finite Temperature*, *Phys. Rev. D* **28** (1983) 340.
- [22] X. Fan, T. G. Myers, B. A. D. Sukra and G. Gabrielse, *Measurement of the Electron Magnetic Moment*, *Phys. Rev. Lett.* **130** (2023) 071801 [[arXiv:2209.13084](#)].
- [23] X. Fan, *An Improved Measurement of the Electron Magnetic Moment*. PhD thesis, Harvard U., 2022.
- [24] A. Hees, O. Minazzoli, E. Savalle, Y. V. Stadnik and P. Wolf, *Violation of the equivalence principle from light scalar dark matter*, *Phys. Rev. D* **98** (2018) 064051 [[arXiv:1807.04512](#)].
- [25] J. Bergé, P. Brax, G. Métris, M. Pernot-Borràs, P. Touboul and J.-P. Uzan, *MICROSCOPE Mission: First Constraints on the Violation of the Weak Equivalence Principle by a Light Scalar Dilaton*, *Phys. Rev. Lett.* **120** (2018) 141101 [[arXiv:1712.00483](#)].
- [26] C. J. Kennedy, E. Oelker, J. M. Robinson, T. Bothwell, D. Kedar, W. R. Milner et al., *Precision Metrology Meets Cosmology: Improved Constraints on Ultralight Dark Matter from Atom-Cavity Frequency Comparisons*, *Phys. Rev. Lett.* **125** (2020) 201302 [[arXiv:2008.08773](#)].
- [27] T. Kobayashi et al., *Search for Ultralight Dark Matter from Long-Term Frequency Comparisons of Optical and Microwave Atomic Clocks*, *Phys. Rev. Lett.* **129** (2022) 241301 [[arXiv:2212.05721](#)].
- [28] NANOGrAV, A. Afzal et al., *The NANOGrav 15 yr Data Set: Search for Signals from New Physics*, *Astrophys. J. Lett.* **951** (2023) L11 [[arXiv:2306.16219](#)].